Hindawi
Complexity
Volume 2022, Article ID 1325825, 9 pages
https://doi.org/10.1155/2022/1325825

Research Article

New Statistical Approaches for Modeling the COVID-19 Data Set: A Case Study in the Medical Sector

Mohammed M. A. Almazah,[1,2] **Kalim Ullah**,[3] **Eslam Hussam**,[4] **Md. Moyazzem Hossain**,[5] **Ramy Aldallal**,[6] **and Fathy H. Riad**[7,8]

[1]*Department of Mathematics, College of Sciences and Arts (Muhyil), King Khalid University, Muhyil 61421, Saudi Arabia*
[2]*Department of Mathematics and Computer, College of Sciences, Ibb University, Ibb 70270, Yemen*
[3]*Foundation University Medical College, Foundation University School of Health Sciences, DHA-I, Islamabad 44000, Pakistan*
[4]*Department of Mathematics, Faculty of Science, Helwan University, Cairo, Egypt*
[5]*Department of Statistics, Jahangirnagar University, Savar, Dhaka 1342, Bangladesh*
[6]*Department of Accounting, College of Business Administration in Hawtat Bani Tamim, Prince Sattam bin Abdulaziz University, Saudi Arabia*
[7]*Mathematics Department, College of Science, Jouf University, P. O. Box 2014, Sakaka, Saudi Arabia*
[8]*Department of Mathematics, Faculty of Science, Minia University, Minia 61519, Egypt*

Correspondence should be addressed to Md. Moyazzem Hossain; hossainmm@juniv.edu

Received 26 May 2022; Revised 27 July 2022; Accepted 3 August 2022; Published 19 August 2022

Academic Editor: Fathalla A. Rihan

Statistical distributions have great applicability for modeling data in almost every applied sector. Among the available classical distributions, the inverse Weibull distribution has received considerable attention. In the practice of distribution theory, numerous methods have been studied and suggested/introduced to increase the flexibility level of the traditional probability distributions. In this paper, we implement different distribution methods to obtain five new different versions of the inverse Weibull model. The new modifications of the inverse Weibull model are called the logarithm transformed-inverse Weibull, a flexible reduced logarithmic-inverse Weibull, the weighted TX-inverse Weibull, a new generalized-inverse Weibull, and the alpha power transformed extended-inverse Weibull distributions. To illustrate the flexibility and applicability of the new modifications of the inverse Weibull model, a biomedical data set is analyzed. The data set consists of 108 observations and represents the mortality rate of the COVID-19-infected patients. The practical application shows that the new generalized-inverse Weibull is the best modification of the inverse Weibull distribution.

1. Introduction

In the practice of distribution theory, one of the important tasks is to devise an efficient statistical model for real phenomena of nature. Generally, the statistical distributions are implemented to analyze real-life situations that are uncertain and endangered. For example, the probability distributions are frequently applied to analyze data in (i) engineering and related sectors [1], (ii) healthcare engineering [2], (iii) the economic and financial sector [3], (iv) hydrology [4], (v) education [5], (vi) metrology [6], (vii) biological sector [7], and (viii) sports [8].

Due to the applicability of the probability distributions in applied areas/sectors, numerous approaches (probability models) have been proposed and studied. For example, Afify et al. [9] proposed the MOPG-Weibull distribution for analyzing the engineering data set. For further studies related to the engineering sector (i.e., data modeling in the engineering-related area), we refer to studies by Almarashi et al. [10] and Strzelecki [11].

Klakattawi [12] implemented a new extended Weibull (NE-Weibull) model for statistical analysis of the data sets related to cancer patients. For more studies related to the biomedical/healthcare data sets (i.e., data modeling in the

biomedical-related area), we refer to studies by Ahmad et al. [13]; Plana et al. [14]; Xin et al. [15]; and Martinez et al. [16].

Tung et al. [17] proposed the arcsine-Weibull (ASin-Weibull) distribution for analyzing data sets in the business and financial sectors. For more studies related to the financial data sets (i.e., data modeling in the financial-related area), we refer to studies by Zhao et al. [18]; Alfaro et al. [19]; Abubakar and Sabri [20]; and Rana et al. [21].

Bakouch et al. [22] implemented the Gumbel model for analyzing the hydrology data set. Singh et al. [23] provided the assessment of groundwater quality data in Nigeria. Hassan et al. [24] implemented the truncated power Lomax (TP-Lomax) distribution for analyzing the flood data set. For other studies related to the hydrology data sets, we refer to studies by Karahacane et al. [25]; Dodangeh et al. [26]; and Tegegne et al. [27].

Among the above fields (engineering, education, hydrology, and healthcare sectors), statistical distributions are frequently implemented to analyze the biomedical data sets. Since December 2019, researchers have proposed and implemented new probability models for analyzing and predicting the COVID-19 events (Baleanu et al. [28]; Özköse and Yavuz, *M*. (2022), Khan et al. [29]; Lella and Pja [30]; Mohan et al. [31]; and Singh et al. [32]).

Maurya et al. [33] proposed a new method called the logarithm transformed (LT) family for introducing flexible probability distributions. Let X has the LT family, if its DF (distribution function) $R(x;\psi)$ is

$$R(x;\boldsymbol{\psi}) = 1 - \frac{\log[2 - M(x;\boldsymbol{\psi})]}{\log 2}, \tag{1}$$

where $x \in \mathbb{R}$ and $M(x;\psi)$ is a baseline DF.

Liu et al. [34] introduced a useful method, namely, a FRL-X (flexible reduced logarithmic-X) family for obtaining the modified versions of the existing distributions. Let X has the FRL-X distributions, if its DF $R(x;\beta,\psi)$ is

$$R(x;\boldsymbol{\psi},\beta) = 1 - \frac{\log[1 - \beta M(x;\boldsymbol{\psi}) + \beta]}{\log(\beta + 1)}, \tag{2}$$

where $\beta \in \mathbb{R}^+$ is an additional parameter.

Ahmad et al. [35] proposed another new class of probability distributions, called the weighted T-X (WT-X) family of distributions. The DF $R(x;\psi)$ of the WT-X distributions is

$$R(x;\boldsymbol{\psi}) = 1 - \frac{1 - M(x;\boldsymbol{\psi})}{e^{M(x;\boldsymbol{\psi})}}, \tag{3}$$

with PDF $r(x;\psi)$ given by

$$r(x;\boldsymbol{\psi}) = [2 - M(x;\boldsymbol{\psi})]\frac{m(x;\boldsymbol{\psi})}{e^{M(x;\boldsymbol{\psi})}}, \tag{4}$$

where $m(x;\psi) = d/dxM(x;\psi)$.

Wang et al. [36] studied a NG-X (new generalized-X) family with DF $R(x;\psi,\theta)$, provided by

$$R(x;\boldsymbol{\psi},\theta) = 1 - e^{-M(x;\boldsymbol{\psi})}[1 - M(x;\boldsymbol{\psi})]^{\theta}, \tag{5}$$

where $\theta \in \mathbb{R}^+$ is the additional parameter.

Bo et al. [37] proposed another useful method, namely, the APTEx-X (alpha power-transformed extended-X) family of distributions. The DF $R(x;\psi,\alpha_1)$ of the APTEx-X family is

$$R(x;\boldsymbol{\psi},\alpha_1) = \frac{\alpha_1^{\left(1-\left(1-M(x;\boldsymbol{\psi})/e^{M(x;\boldsymbol{\psi})}\right)\right)} - 1}{\alpha_1 - 1}, \tag{6}$$

where $\alpha_1 \neq 1, \alpha_1 \in \mathbb{R}^+$ is an additional parameter.

In the next section, we obtain different modifications of the inverse Weibull (IW) distribution by implementing the approaches defined in Eqs. (1)–(6). For every new modified form of the IW model, the plots of the PDF are also obtained.

2. Some New Modifications of the Inverse Weibull Distribution

This section offers some new different extensions of the IW distribution by incorporating the well-known approaches described in Section 1. Consider the DF $M(x;\psi)$, PDF $m(x;\psi)$, SF (survival function) $S(x;\psi)$, HF (hazard function) $h(x;\psi)$, and cumulative HF $H(x;\psi)$ of the IW distribution (with parameters $\alpha \in \mathbb{R}^+$ and $\psi \in \mathbb{R}^+$) given by

$$\begin{aligned} M(x;\boldsymbol{\psi}) &= e^{-\psi/x^{\alpha}}, \\ m(x;\boldsymbol{\psi}) &= \frac{\alpha\psi}{x^{\alpha+1}}e^{-(\psi/x^{\alpha})}, \\ S(x;\boldsymbol{\psi}) &= 1 - e^{-(\psi/x^{\alpha})}, \\ h(x;\boldsymbol{\psi}) &= \frac{\left(\alpha\psi/x^{\alpha+1}\right)}{e^{-(\psi/x^{\alpha})}\left(1 - e^{-(\psi/x^{\alpha})}\right)}, \end{aligned} \tag{7}$$

$$H(x;\boldsymbol{\psi}) = -\log\left(1 - e^{-(\psi/x^{\alpha})}\right), \tag{8}$$

respectively, where $\psi = (\alpha,\psi)$.

2.1. The Logarithm Transformed-Inverse Weibull Distribution. Here, we implement the LT family approach (see (1)) to introduce a new version of the IW model. The new version of the IW model is called the logarithmic transformed-inverse Weibull (LT-IW) distribution. The DF of the LT-IW distribution is obtained by using (7) in (1). Let X has the LT-IW model, if its DF is expressed by

$$R(x;\boldsymbol{\psi}) = 1 - \frac{\log\left[2 - e^{-(\psi/x^{\alpha})}\right]}{\log 2}, \quad x \in \mathbb{R}^+, \alpha, \delta \in \mathbb{R}^+. \tag{9}$$

Associating to Eq. (9), the PDF $r(x;\psi)$, SF $\overline{R}(x;\psi)$, and HF $h(x;\psi)$ of the LT-IW model are given by

$$r(x;\psi) = \frac{\left(\alpha\psi/x^{\alpha+1}\right)e^{-\left(\psi/x^{\alpha}\right)}}{(\log 2)\left[2 - e^{-\left(\psi/x^{\alpha}\right)}\right]},$$

$$\overline{R}(x;\psi) = \frac{\log\left[2 - e^{-\left(\psi/x^{\alpha}\right)}\right]}{\log 2}, \tag{10}$$

$$h(x;\psi) = \frac{\left(\alpha\psi/x^{\alpha+1}\right)e^{-\left(\psi/x^{\alpha}\right)}}{\left(\log\left[2 - e^{-\left(\psi/x^{\alpha}\right)}\right]\right)\left[2 - e^{-\left(\psi/x^{\alpha}\right)}\right]}, \tag{11}$$

respectively.

The PDF plots of the LT-IW model are provided in Figure 1. The plots of the LT-IW model in Figure 1 are obtained for $\alpha = 0.2, \psi = 0.5$ (red line), $\alpha = 3.4, \psi = 0.4$ (green line), $\alpha = 2.5, \psi = 0.5$ (black line), and $\alpha = 2.1, \psi = 1.5$ (blue line).

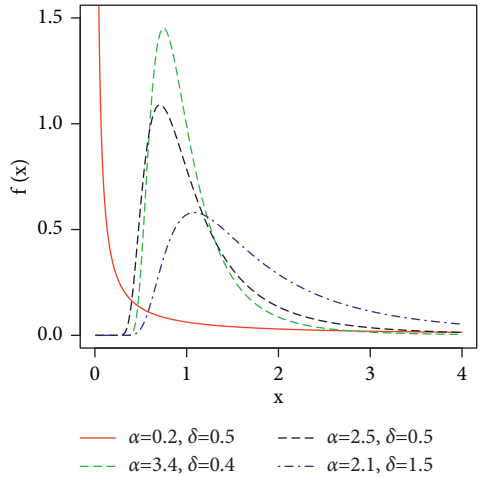

Figure 1: PDF plots of the LT-IW distribution.

2.2. A Flexible Reduced Logarithmic-Inverse Weibull Distribution. Here, we use the FRL-X approach (see (2)) to introduce a novel generalized version of the IW distribution. The new updated form of the IW distribution is called the FRL-IW distribution. The DF of the FRL-IW model is obtained by using Eq. (7) in (2). Let X has the FRL-IW distribution, if its DF is given by

$$R(x;\psi,\beta) = 1 - \frac{\log\left[1 - \beta e^{-\left(\psi/x^{\alpha}\right)} + \beta\right]}{\log(\beta + 1)}, \tag{12}$$

$$x \in \mathbb{R}^{+}, \alpha, \psi, \beta \in \mathbb{R}^{+}.$$

Corresponding to Eq. (12), the PDF $r(x;\beta,\psi)$, SF $\overline{R}(x;\beta,\psi)$, and HF $h(x;\beta,\psi)$ of the FRL-IW model are given by

$$r(x;\beta,\psi) = \frac{\beta\left(\alpha\psi/x^{\alpha+1}\right)e^{-\left(\psi/x^{\alpha}\right)}\left[\log(1+\beta)\right]^{-1}}{\left[1 + \beta - \beta e^{-\left(\psi/x^{\alpha}\right)}\right]},$$

$$\overline{R}(x;\beta,\psi) = \log\left[1 + \beta - \beta e^{-\left(\psi/x^{\alpha}\right)}\right]\left[\log(1+\beta)\right]^{-1}, \tag{13}$$

$$h(x;\beta,\psi) = \frac{\beta\left(\alpha\psi/x^{\alpha+1}\right)e^{-\left(\psi/x^{\alpha}\right)}}{\left(\log\left[1 + \beta - \beta e^{-\left(\psi/x^{\alpha}\right)}\right]\right)\left[1 + \beta - \beta e^{-\left(\psi/x^{\alpha}\right)}\right]}, \tag{14}$$

respectively.

Different plots of $r(x;\beta,\psi)$ of the FRL-IW distribution are presented in Figure 2. The plots of $r(x;\beta,\psi)$ in Figure 2 are obtained for $\alpha = 1.2, \psi = 0.4, \beta = 1.2$ (red line), $\alpha = 3.4$, $\psi = 0.7, \beta = 2.5$ (green line), $\alpha = 2.5, \psi = 0.9, \beta = 2.8$ (black line), and $\alpha = 3.1, \psi = 0.3, \beta = 0.9$ (blue line).

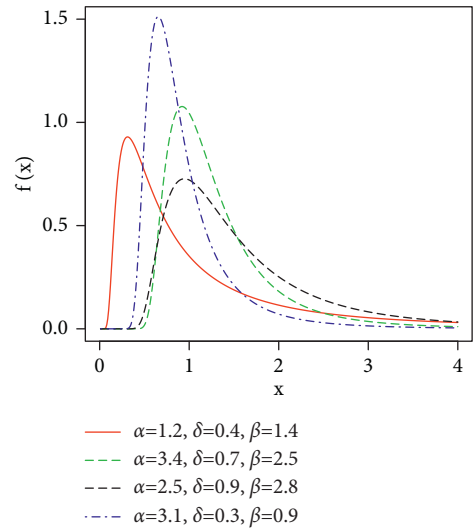

Figure 2: Different plots $r(x;\beta,\psi)$ of the FRL-IW distribution.

2.3. The Weigted TX-Inverse Weibull Distribution. In this section, we apply the WT-X distribution approach to propose a modified version of the IW distribution, called the weighted TX-inverse Weibull (WT X-IW) distribution. The DF of the WT X-IW distribution is obtained by using Eq. (7) in (3). Let X has the WT X-IW model, if its DF is

$$R(x;\psi) = 1 - \frac{1 - e^{-\left(\psi/x^{\alpha}\right)}}{e^{e^{-\left(\psi/x^{\alpha}\right)}}}, \quad x \in \mathbb{R}^{+}, \alpha, \psi \in \mathbb{R}^{+}. \tag{15}$$

In link to (15), the PDF $r(x;\psi)$, SF $\overline{R}(x;\psi)$, and HF $h(x;\psi)$ of the WT X-IW model are given by

$$r(x;\psi) = \left[2 - e^{-\left(\psi/x^{\alpha}\right)}\right]\frac{\left(\alpha\psi/x^{\alpha+1}\right)e^{-\left(\psi/x^{\alpha}\right)}}{e^{e^{-\left(\psi/x^{\alpha}\right)}}},$$

$$\overline{R}(x;\psi) = \frac{1 - e^{-\left(\psi/x^{\alpha}\right)}}{e^{e^{-\left(\psi/x^{\alpha}\right)}}}, \tag{16}$$

$$h(x;\psi) = \left[2 - e^{-\psi/x^{\alpha}}\right]\frac{\left(\alpha\psi/x^{\alpha+1}\right)e^{-\left(\psi/x^{\alpha}\right)}}{1 - e^{-\left(\psi/x^{\alpha}\right)}}, \tag{17}$$

respectively.

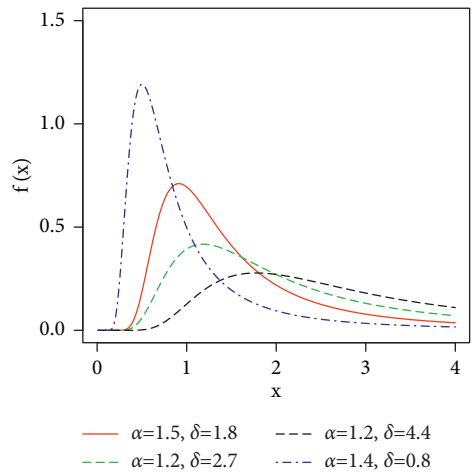

Figure 3: Some possible plots for the PDF of the WTX-IW distribution.

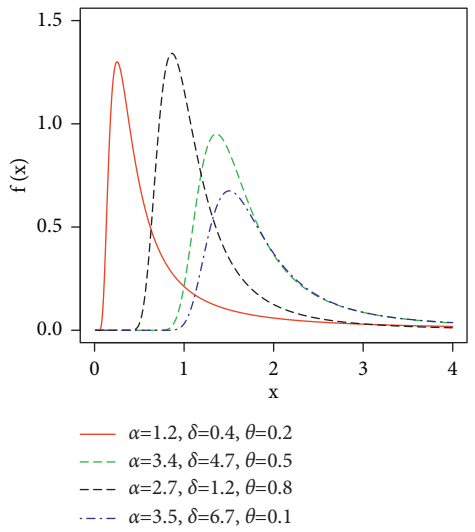

Figure 4: Some possible PDF plots of the NG-IW distribution.

Some possible plots for the PDF of the WTX-IW model are sketched in Figure 3. The plots in Figure 3 are sketched for $\alpha = 1.5, \psi = 1.8$ (red line), $\alpha = 1.2, \psi = 2.7$ (green line), $\alpha = 1.2, \psi = 4.4$ (black line), and $\alpha = 1.4, \psi = 0.8$ (blue line).

2.4. A New Generalized-Inverse Weibull Distribution. In this section, we incorporate a NG-X method and introduce another extended form of the IW distribution. The new extended form of the IW model is called a NG-IW (new generalized-inverse Weibull) model. The DF of the NG-IW model is obtained by using Eq. (7) in (5). Let X has the NG-IW model, if its DF is given by

$$R(x;\theta,\psi) = 1 - \frac{\left[1 - e^{-(\psi/x^{\alpha})}\right]^{\theta}}{e^{e^{-(\psi/x^{\alpha})}}}, \quad x \in \mathbb{R}^{+}, \alpha, \psi, \theta \in \mathbb{R}^{+}. \tag{18}$$

In link to (8), the PDF $r(x;\theta,\psi)$, SF $\overline{R}(x;\theta,\psi)$, and HF $h(x;\theta,\psi)$ of the NG-IW model are, respectively, given by

$$r(x;\theta,\psi) = \frac{\alpha\psi e^{-(\psi/x^{\alpha})}}{x^{\alpha+1}}\left[1 - e^{-(\psi/x^{\alpha})}\right]^{\theta-1}\frac{\left[(1+\theta) - e^{-(\psi/x^{\alpha})}\right]}{e^{e^{-(\psi/x^{\alpha})}}},$$

$$\overline{R}(x;\theta,\psi) = \frac{\left[1 - e^{-(\psi/x^{\alpha})}\right]^{\theta}}{e^{e^{-(\psi/x^{\alpha})}}}, \tag{19}$$

$$h(x;\theta,\psi) = \frac{\alpha\psi e^{-(\psi/x^{\alpha})}}{x^{\alpha+1}\left[1 - e^{-(\psi/x^{\alpha})}\right]}\left[(1+\theta) - e^{-(\psi/x^{\alpha})}\right]. \tag{20}$$

Some possible PDF $r(x;\theta,\psi)$ plots of the NG-IW distribution are sketched in Figure 4. The plots of $r(x;\theta,\psi)$ in Figure 4 are sketched for $\alpha = 1.2, \psi = 0.4, \theta = 0.2$ (red line), $\alpha = 3.4, \psi = 4.7, \theta = 0.5$ (green line), $\alpha = 2.7, \psi = 1.2, \theta = 0.8$ (black line), and $\alpha = 3.5, \psi = 6.7, \theta = 0.1$ (blue line).

2.5. The Alpha Power-Transformed Extended-Inverse Weibull Distribution. This section offers another new extension/generalization of the IW model called the alpha power transformed extended-inverse Weibull (APTE-IW) model. The DF of the APTE-IW distribution is obtained by using Eq. (7) in (6). Let X has the APTE-IW model, if its DF is

$$R(x;\alpha_1,\psi) = \frac{\alpha_1^{\left(1-1-e^{-(\psi/x^{\alpha})}/e^{e^{-(\psi/x^{\alpha})}}\right)} - 1}{\alpha_1 - 1}, \tag{21}$$

$$x \in \mathbb{R}^{+}, \alpha_1 \neq 1, \alpha_1, \alpha, \delta \in \mathbb{R}^{+}.$$

In link to (21), the PDF $r(x;\alpha_1,\psi)$, SF $\overline{R}(x;\alpha_1,\psi)$, and HF $h(x;\alpha_1,\psi)$ of the APTE-IW model are given by

$$r(x;\alpha_1,\psi) = \frac{(\log\alpha)\alpha\psi/x^{\alpha+1}e^{-(\psi/x^{\alpha})}\alpha_1^{\left(1-\left(1-e^{-(\psi/x^{\alpha})}/e^{e^{-(\psi/x^{\alpha})}}\right)\right)}}{(\alpha_1 - 1)\left[2 - e^{-(\psi/x^{\alpha})}\right]^{-1}},$$

$$\overline{R}(x;\alpha_1,\psi) = \frac{\alpha_1 - \alpha_1^{\left(1-\left(1-e^{-(\psi/x^{\alpha})}/e^{e^{-(\psi/x^{\alpha})}}\right)\right)}}{\alpha_1 - 1}, \tag{22}$$

$$h(x;\alpha_1,\psi) = \frac{(\log\alpha)\left(\alpha\psi/x^{\alpha+1}\right)e^{-(\psi/x^{\alpha})}\alpha_1^{\left(1-1-e^{-(\psi/x^{\alpha})}/e^{e^{-(\psi/x^{\alpha})}}\right)}}{\left(\alpha_1 - \alpha_1^{\left(1-1-e^{-(\psi/x^{\alpha})}/e^{e^{-(\psi/x^{\alpha})}}\right)}\right)\left[2 - e^{-(\psi/x^{\alpha})}\right]^{-1}}, \tag{23}$$

respectively.

Some possible PDF $r(x;\alpha_1,\psi)$ plots of the APTE-IW distribution are provided in Figure 5. The plots of $r(x;\alpha_1,\psi)$ in Figure 5 are sketched for $\alpha = 1.2, \psi = 2.1, \theta = 2.2$ (red line), $\alpha = 1.5, \psi = 0.8, \theta = 3.2$ (green line), $\alpha = 1.7, \psi = 1.2, \theta = 3.8$ (black line), and $\alpha = 1.8, \psi = 2.1, \theta = 2.1$ (blue line).

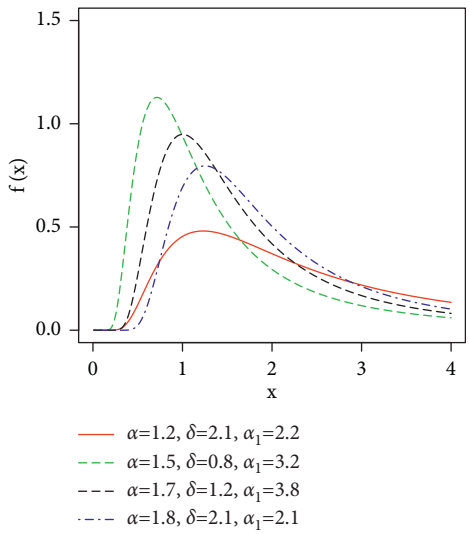

FIGURE 5: Some possible PDF plots of the APTE-IW distribution.

3. Data Analysis

Here, we demonstrate the applicability of the updated versions of the IW distribution. All the proposed updated versions of the IW distribution are applied to a data set concerned with the COVID-19 pandemic. These data are recorded between March 4, 2022, and July 20, 2020 [38].

The considered data set has one hundred eight observations and is given by 1.041, 1.205, 1.402, 1.800, 1.815, 1.923, 2.058, 2.065, 2.070, 2.077, 2.326, 2.352, 2.438, 2.500, 2.506, 2.601, 2.926, 2.988, 3.027, 3.029, 3.215, 3.218, 3.219, 3.228, 3.233, 3.257, 3.286, 3.298, 3.327, 3.336, 3.359, 3.395, 3.440, 3.499, 3.537, 3.632, 3.751, 3.778, 3.922, 4.089, 4.120, 4.292, 4.344, 4.424, 4.557, 4.648, 4.661, 4.697, 4.730, 4.909, 4.949, 5.143, 5.242, 5.317, 5.392, 5.406, 5.442, 5.459, 5.854, 5.985, 6.015, 6.105, 6.122, 6.140, 6.182, 6.327, 6.370, 6.412, 6.535, 6.560, 6.625, 6.656, 6.697, 6.814, 6.968, 7.151, 7.260, 7.267, 7.486, 7.630, 7.840, 7.854, 7.903, 8.108, 8.325, 8.551, 8.696, 8.813, 8.826, 9.284, 9.391, 9.550, 9.935, 10.035, 10.043, 10.158, 10.383, 10.685, 10.855, 11.665, 12.042, 12.878, 13.220, 14.604, 14.962, and 16.498.

The summary values of the COVID-19 data are given by minimum = 1.041, maximum = 16.498, range = 15.457, mean = 5.822, variance = 10.56173, standard derivation- = 3.249882, skewness = 0.9732453, 1^{st} quartile = 3.289, $2^{n\,d}$ quartile or median = 5.279, $3^{r\,d}$ quartile = 7.594, interquartile range = 4.305, and kurtosis = 3.666136. Furthermore, some summary plots of the data set are presented in Figure 6.

Here, we consider four frequently used analytical measures (statistical tests or statistical procedures) to show which probability distribution better fits the biomedical data. These measures are given by the following:

(i) The AIC:

$$\text{AIC} = 2p - 2\pi(\mathbf{\upsilon}). \tag{24}$$

(ii) The BIC:

$$\text{BIC} = p\,\log(m) - 2\pi(\mathbf{\upsilon}). \tag{25}$$

(iii) The CAIC:

$$\text{CAIC} = \frac{2mp}{m-p-1} - 2\pi(\mathbf{\upsilon}). \tag{26}$$

(iv) The HQIC:

$$\text{HQIC} = 2p\,\log(\log(m)) - 2\pi(\mathbf{\upsilon}). \tag{27}$$

In a general sense, the above-mentioned analytical measures are used for comparative analysis. A statistical model that has smaller values of the statistical tests is considered the most suitable model among other competing statistical models.

Table 1 gives the MLEs $(\widehat{\alpha}_{MLE}, \widehat{\psi}_{MLE}, \widehat{\beta}_{MLE}, \widehat{\theta}_{MLE}, \widehat{\alpha_1}_{MLE})$ of the competitive probability models using the COVID-19 data set. The analytical measures for the COVID-19 data using the considered probability models are presented in Table 2.

Based on the reported results in Table 2, it is obvious that the NG-IW model provides the best fit to the biomedical data. For the NG-IW model, the values of the considered test statistics are AIC = 531.7657, CAIC = 532.0010, BIC = 539.7561, and HQIC = 535.0043. Based on the numerical results in Table 2, the second appropriate model is the FRL-IW distribution. For the FRL-IW model, we have AIC = 546.7329, CAIC = 546.9682, BIC = 554.7232, and HQIC = 549.9714. The $3^{r\,d}$ best model is the LT-IW distribution. For the LT-IW model, AIC = 549.0155, CAIC = 549.1321, BIC = 554.3424, and HQIC = 551.1746. The 4^{th} best model is the WTX-IW distribution. For the WTX-IW model, AIC = 551.7866, CAIC = 551.9032, BIC = 557.1135, and HQIC = 553.9457. The 5^{th} best model is the APTE-IW distribution. For the APTE-IW model, AIC = 553.3800, CAIC = 553.6043, BIC = 561.5085, and HQIC = 556.6775.

As we have seen that the NG-IW model provides a close fit to the biomedical data. Therefore, we provide the profiles of the log-likelihood function (LLF) of the NG-IW distribution. Based on the $\widehat{\alpha}_{MLE}$, $\widehat{\psi}_{MLE}$, and $\widehat{\theta}_{MLE}$, the LLF profiles of the NG-IW distribution are obtained in Figure 7. The graphs in Figure 7 confirm the unique values of the $\widehat{\alpha}_{MLE}$, $\widehat{\psi}_{MLE}$, and $\widehat{\theta}_{MLE}$.

After the numerical illustration of the NG-IW model using the COVID-19 data set (see Table 2), next we show visually that the NG-IW model provides the best fit to the COVID-19 data set. For the visual illustration of the NG-IW model, the plots of the fitted PDF $r(x;\widehat{\theta},\widehat{\psi})$, DF $R(x;\widehat{\theta},\widehat{\psi})$, SF $\overline{R}(x;\widehat{\theta},\widehat{\psi})$, HF $h(x;\widehat{\theta},\widehat{\psi})$, cumulative HF $H(x;\widehat{\theta},\widehat{\psi})$, probability-probability (PP), and QQ (quantile-quantile) are obtained in Figure 8. The plots of $r(x;\widehat{\theta},\widehat{\psi})$, $R(x;\widehat{\theta},\widehat{\psi})$, $\overline{R}(x;\widehat{\theta},\widehat{\psi})$, $h(x;\widehat{\theta},\widehat{\psi})$, and $H(x;\widehat{\theta},\widehat{\psi})$ are obtained using the following expressions:

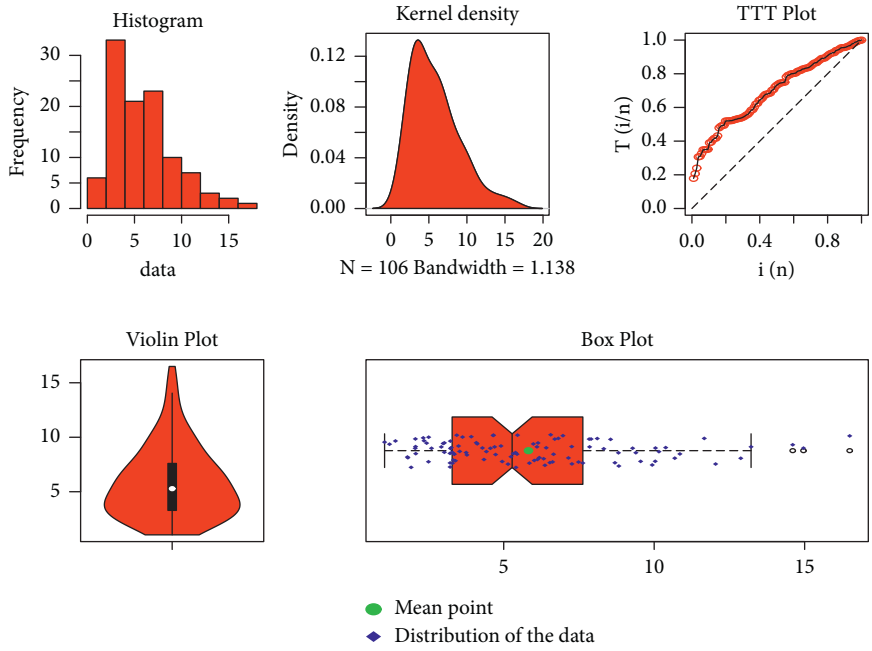

Figure 6: Some summary plots of the COVID-19 data set.

Table 1: The values of the maximum likelihood estimators of the fitted models using the COVID-19 data set.

Distributions	$\widehat{\alpha}$	$\widehat{\psi}$	$\widehat{\beta}$	$\widehat{\theta}$	$\widehat{\alpha}_1$
LT-IW	1.829195	8.721454	—	—	—
FRL-IW	2.291612	8.003594	11.582096	—	—
WTX-IW	1.339224	9.164487	—	—	—
NG-IW	0.705908	8.586715	—	9.655237	—
APTE-IW	0.633391	8.119927	—	—	12.65028

Table 2: The values of the analytical measures of the fitted models using the COVID-19 data set.

Distributions	AIC	CAIC	BIC	HQIC
LT-IW	549.0155	549.1321	554.3424	551.1746
FRL-IW	546.7329	546.9682	554.7232	549.9714
WTX-IW	551.7866	551.9032	557.1135	553.9457
NG-IW	531.7657	532.0010	539.7561	535.0043
APTE-IW	553.3800	553.6043	561.5085	556.6775

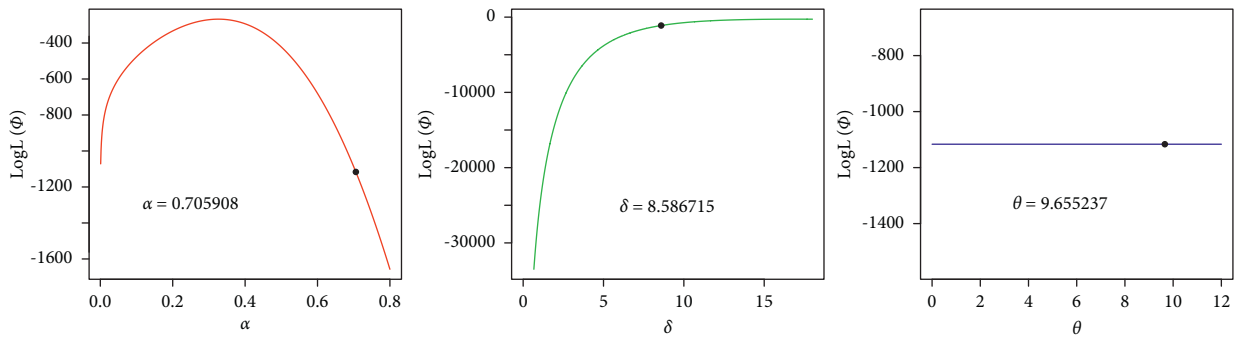

Figure 7: The profiles of the log LF of the NG-IW distribution using the COVID-19 data set.

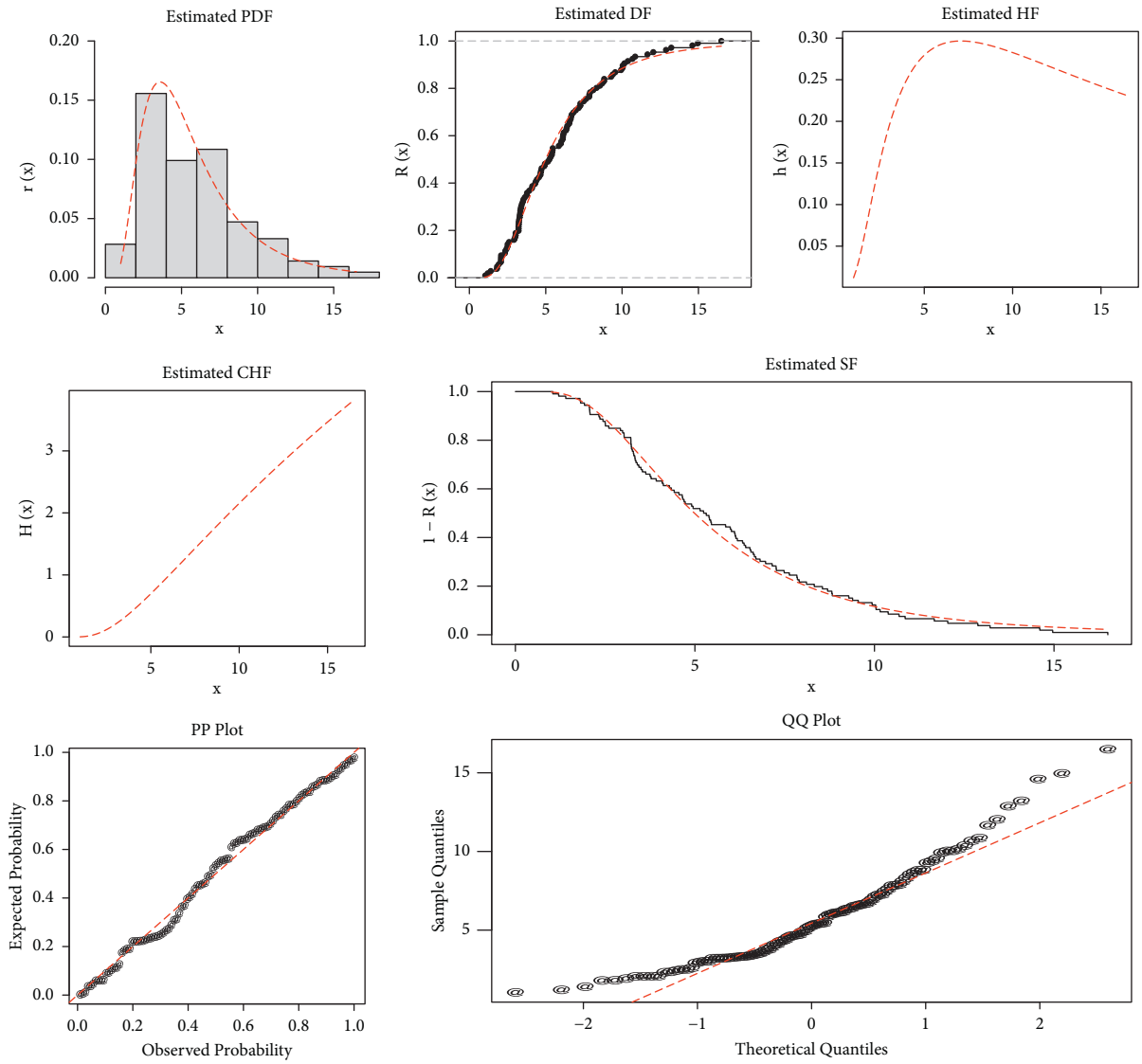

Figure 8: Visual illustration of the NG-IW distribution using the COVID-19 data set.

$$
\begin{aligned}
r(x;\widehat{\theta},\widehat{\psi}) &= \frac{6.061430\, e^{-8.586715/x^{0.705908}}}{x^{1.705908}}\left[1-e^{-8.586715/x^{0.705908}}\right]^{8.655237} \times \frac{\left[(10.655237)-e^{-8.586715/x^{0.705908}}\right]}{e^{e^{-8.586715/x^{0.705908}}}},\\
R(x;\widehat{\theta},\widehat{\psi}) &= 1-\frac{\left[1-e^{-8.586715/x^{0.705908}}\right]^{9.655237}}{e^{e^{-8.586715/x^{0.705908}}}},\\
\overline{R}(x;\widehat{\theta},\widehat{\psi}) &= \frac{\left[1-e^{-8.586715/x^{0.705908}}\right]^{9.655237}}{e^{e^{-8.586715/x^{0.705908}}}},\\
h(x;\theta,\psi) &= \frac{6.061430\, e^{-8.586715/x^{0.705908}}}{x^{1.705908}\left[1-e^{-8.586715/x^{0.705908}}\right]}\left[(10.655237)-e^{-8.586715/x^{0.705908}}\right],
\end{aligned}
\tag{28}
$$

$$
H(x;\widehat{\theta},\widehat{\psi}) = -\log\left(\frac{\left[1-e^{-8.586715/x^{0.705908}}\right]^{9.655237}}{e^{e^{-8.586715/x^{0.705908}}}}\right),
\tag{29}
$$

respectively.

The empirical and fitted plots in Figure 8 reveal that the NG-IW distribution provides a close fit to the COVID-19 data set.

4. Concluding Remarks

In recent times, statistical models have been frequently used to analyze data in applied sectors, such as engineering, hydrology, education, finance, and biomedical sectors. To provide the best description of the phenomena under consideration, a number of statistical models have been introduced and implemented. Among these models, the IW distribution has received considerable attention. Therefore, numerous modifications of the IW distribution have been proposed and applied. In this paper, we introduced five different modifications of the IW distribution for modeling real-life data sets. Finally, the new modified forms of the IW distribution were applied to real-life data taken from the biomedical sector. The practical application showed that the NG-IW distribution was the best candidate model for analyzing the COVID-19 data set.

In the future, we are motivated to implement the LT-IW, FRL-IW, WTX-IW, NG-IW, and APTE-IW models in other applied sectors. Furthermore, the bivariate extensions of the LT-IW, FRL-IW, WTX-IW, NG-IW, and APTE-IW models can also be introduced to deal with the bivariate data sets. Bayesian estimation of the LT-IW, FRL-IW, WTX-IW, NG-IW, and APTE-IW models using different types of censored samples can be discussed [39].

Data Availability

All data are included in the paper.

Conflicts of Interest

The authors declare no conflicts of interest.

Acknowledgments

The first author acknowledges the support of Deanship of Scientific Research at King Khalid University for funding this work through Larg Groups (a project under grant no. RGP.2/34/43).

References

[1] L. Pan, L. Novák, D. Lehký, D. Novák, and M. Cao, "Neural network ensemble-based sensitivity analysis in structural engineering: comparison of selected methods and the influence of statistical correlation," *Computers & Structures*, vol. 242, Article ID 106376, 2021.

[2] E. Gholipour, B. Vizvári, T. Babaqi, and S. Takács, "Statistical analysis of the Hungarian COVID-19 victims," *Journal of Medical Virology*, vol. 93, no. 12, pp. 6660–6670, 2021.

[3] S. Dutta and K. Saini, "Statistical assessment of hybrid blockchain for SME sector," *WSEAS Transactions on Systems and Control*, vol. 16, pp. 83–95, 2021.

[4] B. Moccia, C. Mineo, E. Ridolfi, F. Russo, and F. Napolitano, "Probability distributions of daily rainfall extremes in Lazio and Sicily, Italy, and design rainfall inferences," *Journal of Hydrology: Regional Studies*, vol. 33, Article ID 100771, 2021.

[5] E. Artigao, A. Vigueras-Rodríguez, A. Honrubia-Escribano, S. Martín-Martínez, and E. Gómez-Lázaro, "Wind resource and wind power generation assessment for education in engineering," *Sustainability*, vol. 13, no. 5, p. 2444, 2021.

[6] M. Aslam, "Testing average wind speed using sampling plan for Weibull distribution under indeterminacy," *Scientific Reports*, vol. 11, no. 1, pp. 7532–7539, 2021.

[7] F. A. Rihan, *Delay Differential Equations and Applications to Biology*, Springer, Singapore, 2021.

[8] G. Shengjie, A. Craig, and G. T. Mekiso, "A new alpha power Weibull model for analyzing time-to-event data: a case study from football," *Mathematical Problems in Engineering*, vol. 2022, pp. 1–10, 2022.

[9] A. Z. Afify, D. Kumar, and I. Elbatal, "Marshall–Olkin power generalized Weibull distribution with applications in engineering and medicine," *Journal of Statistical Theory and Applications*, vol. 19, no. 2, pp. 223–237, 2020.

[10] A. M. Almarashi, A. Algarni, and M. Nassar, "On estimation procedures of stress-strength reliability for Weibull distribution with application," *PLoS One*, vol. 15, no. 8, Article ID e0237997, 2020.

[11] P. Strzelecki, "Determination of fatigue life for low probability of failure for different stress levels using 3-parameter Weibull distribution," *International Journal of Fatigue*, vol. 145, Article ID 106080, 2021.

[12] H. S. Klakattawi, "Survival analysis of cancer patients using a new extended Weibull distribution," *PLoS One*, vol. 17, no. 2, Article ID e0264229, 2022.

[13] Z. Ahmad, Z. Almaspoor, F. Khan, and M. El-Morshedy, "On predictive modeling using a new flexible Weibull distribution and machine learning approach: analyzing the COVID-19 data," *Mathematics*, vol. 10, no. 11, p. 1792, 2022.

[14] D. Plana, G. Fell, B. M. Alexander, A. C. Palmer, and P. K. Sorger, "Cancer patient survival can be parametrized to improve trial precision and reveal time-dependent therapeutic effects," *Nature Communications*, vol. 13, no. 1, pp. 873–913, 2022.

[15] Y. Xin, Y. Zhou, and G. T. Mekiso, "A New Generalized-Family for Analyzing the COVID-19 Data Set: a Case Study," *Mathematical Problems in Engineering*, p. 1, Article ID 1901526, 2022.

[16] E. Z. Martinez, B. C. L. de Freitas, J. A. Achcar, D. C. Aragon, and M. V. de Oliveira Peres, "Exponentiated Weibull models applied to medical data in presence of right-censoring, cure fraction and covariates. Statistics," *Optimization & Information Computing*, vol. 10, no. 2, pp. 548–571, 2022.

[17] Y. Liang Tung, Z. Ahmad, and E. Mahmoudi, "The arcsine-X family of distributions with applications to financial sciences," *Computer Systems Science and Engineering*, vol. 39, no. 3, pp. 351–363, 2021.

[18] W. Zhao, S. K. Khosa, Z. Ahmad, M. Aslam, and A. Z. Afify, "Type-I heavy tailed family with applications in medicine, engineering and insurance," *PLoS One*, vol. 15, no. 8, Article ID e0237462, 2020.

[19] N. M. Alfaer, A. M. Gemeay, H. M. Aljohani, and A. Z. Afify, "The extended log-logistic distribution: inference and actuarial applications," *Mathematics*, vol. 9, no. 12, p. 1386, 2021.

[20] H. Abubakar and S. R. M. Sabri, "A simulation study on modified Weibull distribution for modelling of investment return," *Pertanika Journal of Science & Technology*, vol. 29, no. 4, pp. 2767–2790, 2021.

[21] M. S. Rana, S. H. Shahbaz, M. Q. Shahbaz, and M. M. Rahman, "Pareto-weibull distribution with properties and applications: a member of pareto-X family," *Pakistan Journal of Statistics and Operation Research*, vol. 18, pp. 121–132, 2022.

[22] H. S. Bakouch, C. Chesneau, and O. A. Elsamadony, "The Gumbel kernel for estimating the probability density function with application to hydrology data," *Journal of Digital Information Management*, vol. 3, no. 4, pp. 261–269, 2021.

[23] V. V. Singh, A. A. Suleman, A. Ibrahim, U. A. Abdullahi, and S. A. Suleiman, "Assessment of probability distributions of groundwater quality data in Gwale area, north-western Nigeria," *Annals of Optimization Theory and Practice*, vol. 3, no. 1, pp. 37–46, 2020.

[24] A. S. Hassan, M. A. Sabry, and A. M. Elsehetry, "Truncated power Lomax distribution with application to flood data," *Journal of Statistics Applications & Probability*, vol. 9, pp. 347–359, 2020.

[25] H. Karahacane, M. Meddi, F. Chebana, and H. A. Saaed, "Complete multivariate flood frequency analysis, applied to northern Algeria," *Journal of Flood Risk Management*, vol. 13, no. 4, Article ID e12619, 2020.

[26] E. Dodangeh, V. P. Singh, B. T. Pham, J. Yin, G. Yang, and A. Mosavi, "Flood frequency analysis of interconnected rivers by copulas," *Water Resources Management*, vol. 34, no. 11, pp. 3533–3549, 2020.

[27] G. Tegegne, A. M. Melesse, D. H. Asfaw, and A. W. Worqlul, "Flood frequency analyses over different basin scales in the Blue Nile River basin, Ethiopia," *Hydrology*, vol. 7, no. 3, p. 44, 2020.

[28] D. Baleanu, M. Hassan Abadi, A. Jajarmi, K. Zarghami Vahid, and J. J. Nieto, "A new comparative study on the general fractional model of COVID-19 with isolation and quarantine effects," *Alexandria Engineering Journal*, vol. 61, no. 6, pp. 4779–4791, 2022.

[29] M. A. Khan, R. Khan, F. Algarni, I. Kumar, A. Choudhary, and A. Srivastava, "Performance evaluation of regression models for COVID-19: a statistical and predictive perspective," *Ain Shams Engineering Journal*, vol. 13, no. 2, Article ID 101574, 2022.

[30] K. K. Lella and A. Pja, "Automatic diagnosis of COVID-19 disease using deep convolutional neural network with multi-feature channel from respiratory sound data: cough, voice, and breath," *Alexandria Engineering Journal*, vol. 61, no. 2, pp. 1319–1334, 2022.

[31] S. Mohan, A. Abugabah, A. Abugabah et al., "An approach to forecast impact of Covid-19 using supervised machine learning model," *Software: Practice and Experience*, vol. 52, no. 4, pp. 824–840, 2022.

[32] P. Singh and A. Gupta, "Generalized SIR (GSIR) epidemic model: an improved framework for the predictive monitoring of COVID-19 pandemic," *ISA Transactions*, vol. 124, pp. 31–40, 2022.

[33] S. K. Maurya, A. Kaushik, R. K. Singh, S. K. Singh, and U. Singh, "A new method of proposing distribution and its application to real data," *Imperial Journal of Interdisciplinary Research*, vol. 2, no. 6, pp. 1331–1338, 2016.

[34] Y. Liu, M. Ilyas, S. K. Khosa et al., "A flexible reduced logarithmic-X family of distributions with biomedical analysis," *Computational and Mathematical Methods in Medicine*, vol. 2020, p. 1, 2020.

[35] Z. Ahmad, E. Mahmoudi, G. G. Hamedani, and O. Kharazmi, "New methods to define heavy-tailed distributions with applications to insurance data," *Journal of Taibah University for Science*, vol. 14, no. 1, pp. 359–382, 2020.

[36] W. Wang, Z. Ahmad, O. Kharazmi, C. B. Ampadu, E. H. Hafez, and M. M. Mohie El-Din, "New generalized-x family: modeling the reliability engineering applications," *PLoS One*, vol. 16, no. 3, Article ID e0248312, 2021.

[37] W. Bo, Z. Ahmad, A. R. Alanzi, A. I. Al-Omari, E. H. Hafez, and S. F. Abdelwahab, "The current COVID-19 pandemic in China: an overview and corona data analysis," *Alexandria Engineering Journal*, vol. 61, no. 2, pp. 1369–1381, 2022.

[38] H. M. Almongy, E. M. Almetwally, H. M. Aljohani, A. S. Alghamdi, and E. H. Hafez, "A new extended Rayleigh distribution with applications of COVID-19 data," *Results in Physics*, vol. 23, Article ID 104012, 2021.

[39] F. Özköse and M. Yavuz, "Investigation of interactions between COVID-19 and diabetes with hereditary traits using real data: a case study in Turkey," *Computers in Biology and Medicine*, vol. 141, Article ID 105044, 2022.